The American Journal of Human Genetics, Volume *109*

Supplemental information

De novo variants in *ATP2B1* lead to neurodevelopmental delay

Meer Jacob Rahimi, Nicole Urban, Meret Wegler, Heinrich Sticht, Michael Schaefer, Bernt Popp, Frank Gaunitz, Manuela Morleo, Vincenzo Nigro, Silvia Maitz, Grazia M.S. Mancini, Claudia Ruivenkamp, Eun-Kyung Suk, Tobias Bartolomaeus, Andreas Merkenschlager, Daniel Koboldt, Dennis Bartholomew, Alexander P.A. Stegmann, Margje Sinnema, Irma Duynisveld, Ramona Salvarinova, Simone Race, Bert B.A. de Vries, Aurélien Trimouille, Sophie Naudion, Daphna Marom, Uri Hamiel, Noa Henig, Florence Demurger, Nils Rahner, Enrika Bartels, J. Austin Hamm, Abbey M. Putnam, Richard Person, Rami Abou Jamra, and Henry Oppermann

SUPPLEMENTAL DATA

SUPPLEMENTAL NOTE: CASE REPORTS

Individual 1

Patient 1 is a 7-year-old girl who is the second child of three, born from healthy and non-consanguineous parents of European origin. The older sister and younger brother are healthy. Pregnancy and delivery were uneventful and birth parameters were within the normal range. Apgar score was 8/9. At birth dysmorphic features, hypotonia and a patent foramen ovale were noted. Karyotype and comparative genomic hybridization microarray (SurePrint G3 Human CGH Microarray 8x60K, Agilent) did not reveal any abnormalities. In the subsequent years a metabolic screening, analysis of *FMR1* gene and *ZEB2* gene (sequencing and MLPA) were normal.

At the last evaluation (age 6 years and 6 months) the patient showed weight -0.56 SD, height -1.00 SD and head circumference -1.83 SD.

Independent walking had been achieved at 21 months. The first words were reported around 30 months. Verbal communication was limited to few unintelligible words, but the girl showed good comprehension and non-verbal communication. Parents reported short attention span. No behavioral abnormalities were noted.

Medical issues comprise interatrial cardiac defect (ostium secundum) and pes planus. She experienced a febrile seizure. A cranial MRI showed a dilatation of the ventricular system

Dysmorphic features were described: coarse facial features, large and anteverted ears with dysmorphic helix, wide nasal bridge and bulbous tip. There is a supernumerary nipple. Clinodactyly of the IV toe bilaterally.

Individual 2

Patient no.2 was born after 39 weeks of pregnancy (unknown length, weight 3240 g (-0.6 SDS)) as a son of a Chinese mother and father, both parents with an unremarkable family history. He is presented with motor developmental delay (unassisted walking with 16 months) and a language development disorder became apparent (first words at 24 months).

He has autism/autism like behavior. The patient exhibits normal growth parameters but has low-set ears with overfolded helix. He was diagnosed with transposition of great vessels and according underwent surgically switch operation at birth. He lives with a residual minor pulmonalis stenosis.

Individual 3

Patient no.3 was born after 37 weeks of pregnancy (unknown length and weight) as a son (twin) of a mother and a father of European descent, both parents with an unremarkable family history. He is presented with motor developmental delay and a language development disorder became apparent.

His EEG was pathologic. A cranial MRI showed a cerebral cavernom. The patient exhibits normal growth parameters, bilateral short achilles tendons and sparse hair.

Individual 4

Patient no.4 was born after 37+3 weeks of pregnancy (length 50 cm (-0.65 SDS), weight 2860 g (-1.05 SDS)) as son of a mother of European descent and a father with Asian ancestry, both parents with an unremarkable family history. In the first year of life he presented with motor developmental delay (unassisted walking with 19 months), during the second year a language development disorder became apparent. At the age of 34 months, according to the Munich functional developmental diagnostic (MFDD) the expressive language and social skills

corresponded to the developmental age of 20 and 18 months, respectively. At that age, an autistic spectrum disorder clearly was determined.

His EEG was pathological due to epileptic discharges at the age of 2 years, first clinical seizures occurred as myoclonias and atypical absences at the age of 3 years and 2 months, a few month later a continuous spike and wave status (CSWS) was found in the sleep EEG. The epilepsy was classified as atypical childhood epilepsy with centrotemporal spikes. Clinical seizures were resistant to antiepileptic drugs: topiramate, levetiracetame, valproate and clobazam; eventually sulthiame led to clinical remission and controlled the electrical status epilepticus. Starting with the age of 6 years the body mass index slowly declined to -4.00 SDS (at the age of 17 years and 1 month length 181.4 cm and weight 41.95 kg) and he developed a distinct marfanoid habitus with arachnodactyly, S-shaped scoliosis and hypermobility of thumb.

Individual 5

This patient was born from non-consanguineous parents, at term with normal APGAR scores. Birthweight was 3,850g. The patient exhibited delayed motor milestones and delayed speech. Furthermore, he has mild ID with autistic features and some facial dysmorphia. Karyotyping at age 3 showed a <20% mosaicism for XXY (Klinefelter). MRI at age 4 showed no abnormalities. IQ tested at age 9: TIQ46, VIQ<55, PIQ<55. Adult length 194cm, armsspan 192cm, OFC 56cm.

Individual 6

The patient is a 5 years-10 months old boy, with treatment resistant epileptic encephalopathy, failure to thrive, visual cortical impairment, sensorineural hearing loss, G-tube , feeding difficulties with irritability and crying, gastroesophageal reflux, and minimally subluxated hips.

He is the 1st child to non-consanguineous parents, born after an unremarkable pregnancy, presenting with infantile spasms at 2 months of age. He has ongoing tonic seizures every 1-2 days and clusters of epileptic spasms daily currently managed with Rufinamide and CBD oil.

The patient has history of aspiration pneumonia. He is exclusively fed via G-tube, with ongoing feeding difficulties and is treated for gastroesophageal reflux disease. He has managed with minimally subluxed hips bilaterally.

Clinical evaluation at age of 2 years revealed mild dysmorphology including: low anterior hairline and a ridge at the line of the coronal suture, flattened occiput, relatively thin, arched eyebrows and long eyelashes, deep set eyes and a prominent forehead, broad nasal root and a bulbous nasal tip, excess nuchal skin and no neck widening. He had fleshy palms, deep palmar creases and subcutaneous adipose creases on the medial aspect of his calves, and above his popliteal fossae bilaterally.

Developmentally the patient shows severe delay and requires full care. In terms of motor skills he is able to roll. He has cortical visual impairment, nystagmus and variable alternating exotropia with a slight optic nerve pallor. He is wearing hearing aids in view of bilateral sensory neural hearing loss.

Biochemical investigations in blood, urine, and CSF were unremarkable. Chromosomal microarray was normal male. Clinical trio exome sequencing with mtDNA sequencing identified *de novo* heterozygous variant c.2365C>T, p.(Arg789Cys) in *ATP2B1*.

Individual 7

This 17 years old girl was born after a normal pregnancy at term with a birth weight of 3500 gram. She developed seizures at the age of 4 months and, subsequently regressed. She was

diagnosed with West syndrome at the age of 6 months. She responded well to Sabril at 10 months and remained free of seizures. She started walking independently and speaking first words at 3 years of age. MRI of the brain revealed no abnormalities and also metabolic studies were normal. Her level was ascertained and she had an IQ of 58. She developed behavior problems with obsessive aspects.

She had a normal growth with height of 175 cm (75th centile) and head circumference of 55.5 cm (25th centile). She did not have any facial dysmorphism.

Whole exome sequencing revealed a *de novo* missense variant in *ATP2B1*, c.2470G>A, p.(Glu824Lys).

Individual 8

Patient no.8 was born after 39 weeks of pregnancy (length 47 cm, weight 3100 g (-0.6 SDS)) as a daughter of a Moroccan mother and father, both parents with an unremarkable family history. She has an older brother in good health. At birth, Apgar score was 6/10, and she needed to be hospitalized for respiratory distress with no known etiology.

During the first year of life, she had been hospitalized for dyspnea with stridor, vomiting, and feeding difficulties.

She is presented with motor developmental delay (sitting with 12 months) and a language development disorder became apparent (first words at 26 months). The patient exhibits normal growth parameters. Clinical examination shows brachycephaly, very low hairline on the forehead, bilateral epicanthus, very long eyelashes, bulbous nasal tip, hat-shaped mouth, ogival palate, and hirsutism. She has low implanted thumbs, deep palmar folds and clinodactyly of the 5th fingers. She also has hepatomegaly with cholestasis. In addition to the *ATP2B1* variant c.2570A>G, p.(Gln857Arg), WES analysis found an additional *WDR83OS*

homozygous variant, possibly involved in the hepatic symptoms: NM_016145.3:c.255-4_260del, p.?.

Individual 9

Patient no.9 is a 51 years old male manifesting a simplex case of early childhood nonprogressive global developmental delay. Later on, he was diagnosed with mild syndromic intellectual disability (IQ 73), learning and behavioral difficulties and high function autism spectrum disorder. He attended special education and is now leading a nearly total independent life, living on his own and being employed. Physical findings include a marfanoid habitus, tall stature 183 cm (80th percentile), head circumference 57.5 cm (75th percentile), arachnodactyly (total hand length and middle finger length 22cm & 13cm both > 97th percentile), low folded soft earlobes, high-arched palate, pectus carinatum, scoliosis, mild DIP and PIP camptodactyly and club foot. Hypertelorism was ruled out. Recent echocardiography revealed mild aortic root dilation but an otherwise structurally normal heart. He has no other congenital anomalies. Hearing and eye examination are normal.

Prior (2014-2016) genetic studies (CMA, Fragile X, maternal X inactivation analysis and singleton clinical exome) were all unremarkable.

Individual 10

Patient no.10 was born after 40 weeks of pregnancy (length 47 cm, weight 2650 g (-2.2 SDS)) as a son of a mother and father of European descent, both parents with an unremarkable family history. He is presented with motor developmental delay and a language development disorder became apparent.

He shows signs of hyperactivity. The patient exhibits normal growth parameters but has some craniofacial abnormalities like sparse eyebrows or palpebral edema.

Individual 11

Patient no.11 was born after 40 weeks of pregnancy (length 52 cm (+0.1 SDS), weight 3450 g (0 SDS)) as a daughter of a mother and father of European descent, both parents are without an education/qualification. The father especially was a late talker (with 7 years). She is presented with a language development disorder became apparent. A SONR 2 1/2-7 non-verbal intelligence test at the age of 4.4 years displayed a cognitive performance as at 2.2 years of age. The patient exhibits a short stature and has no other abnormalities.

Individual 12

Patient no.12 is a 5 year old son of a Chinese mother and father, both parents with an unremarkable family history. He is presented with motor developmental delay (unassisted walking with 21 months) and is nonambulatory and nonverbal.

He experienced infantile spasms. A cranial MRI showed a small area of gliosis or encephalomalacia of the left caudate nucleus. Furthermore, he has autism/autism like behavior and lives with anxiety, sleeping and mood problems. The patient exhibits normal growth parameters but has esotropia and plagiocepahly. He has some congenital malformations like PFO, cryptorchidism, hypospadias, pectus excavatum and sacral dimple.

Individual 16 (excluded from the clinical description)

Individual 16 is a 5-year-old male (born Aug 2016) of European ancestry. He came to medical attention during the prenatal period when an ultrasound noted bilateral CL/P and significant

oligohydramnios. He was born at term but admitted to the NICU due to feeding issues and apneic spells. He was referred to clinical genetics at 17 months of age for evaluation of multiple issues including failure to thrive, hypotonia, developmental delay, dysmorphic features, and a single seizure (at age 4 months). He had a striking macrocephaly (>99th percentile) and CL/P (surgically repaired), both of which were present in his mother. He was also noted for triangular facies, slight ptosis, inferior inner epicanthal folds, and downslanting palpebral fissures. His most recent brain MRI (2019) was normal, and his seizures (generalized tonic-clonic seizures of unknown etiology) have been under control with Keppra. Though noted for poor intestinal motility, his appetite has improved. He has ongoing developmental delays and receives physical, occupational, and speech therapies. After a non-diagnostic clinical WES (2018), he was referred for further genomic studies under an IRB-approved research study at Nationwide Children's Hospital. Trio whole-genome sequencing revealed a *de novo* variant in *ATP2B1*, NM_001682.3:c.1793T>C, p.(Ile598Thr), which was confirmed by Sanger sequencing. Structural protein modeling suggested that this variant not critically affect ATP2B1 structure, as Ile598 is rather solvent exposed. Furthermore, the membrane localization (0.57±0.11; wild-type:0.6±0.07; $p>0.05$) and the tau-vale (12.67±1.33; wild-type:12.66±1.41; $p>0.05$) of p.Ile598Thr was indistinguishable from the wild-type. Thus, as the relevance of this variant is uncertain, we excluded this individual from the phenotypic analysis.

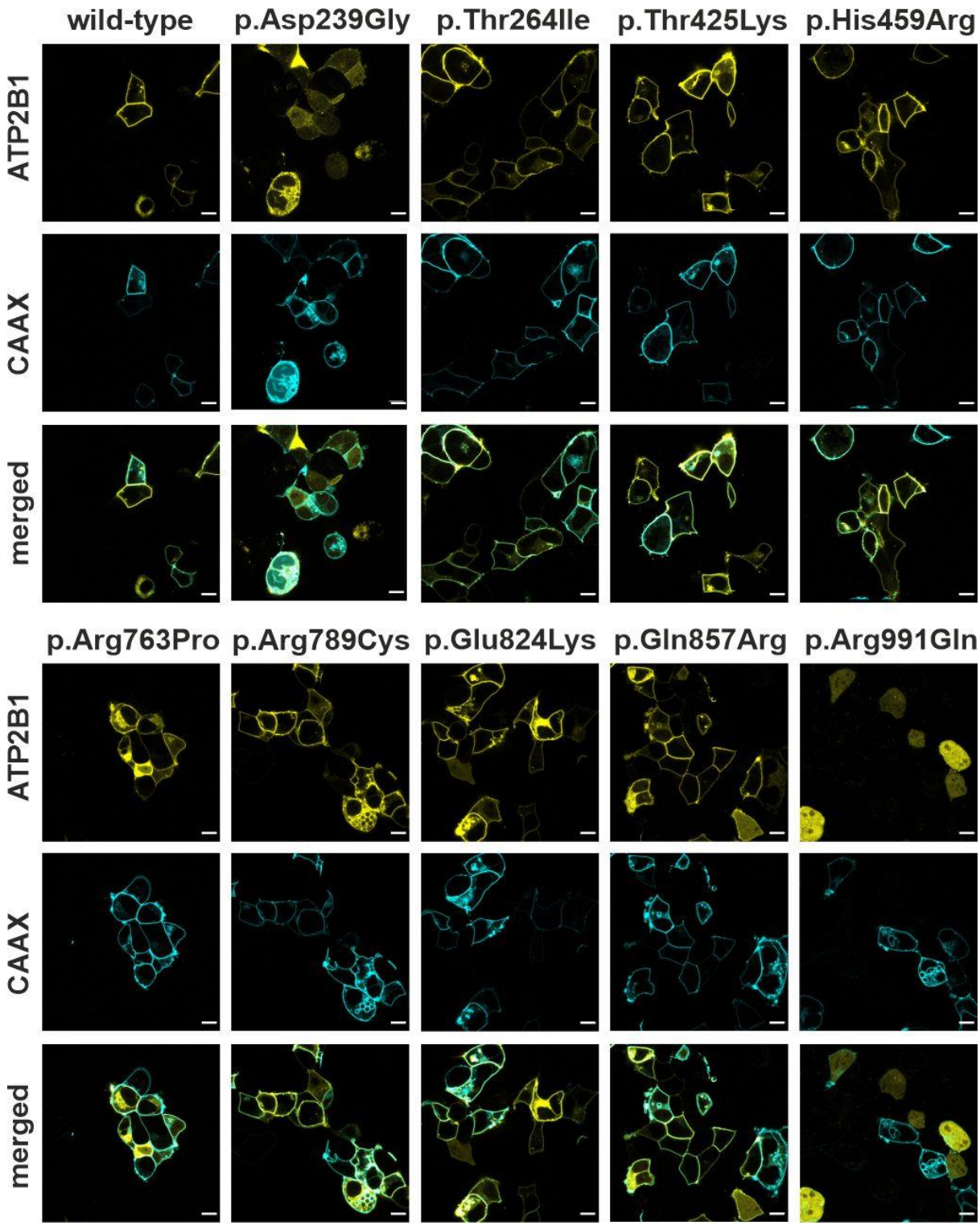

Figure S1: Subcellular localization of transiently overexpressed *ATP2B1* variants. (A) Representative confocal laser scanning microscopy images of transfected HEK293 cells expressing YFP-fused ATP2B1 and a CAAX-box-modified cyan fluorescent protein. Scale bars: 10 µm.

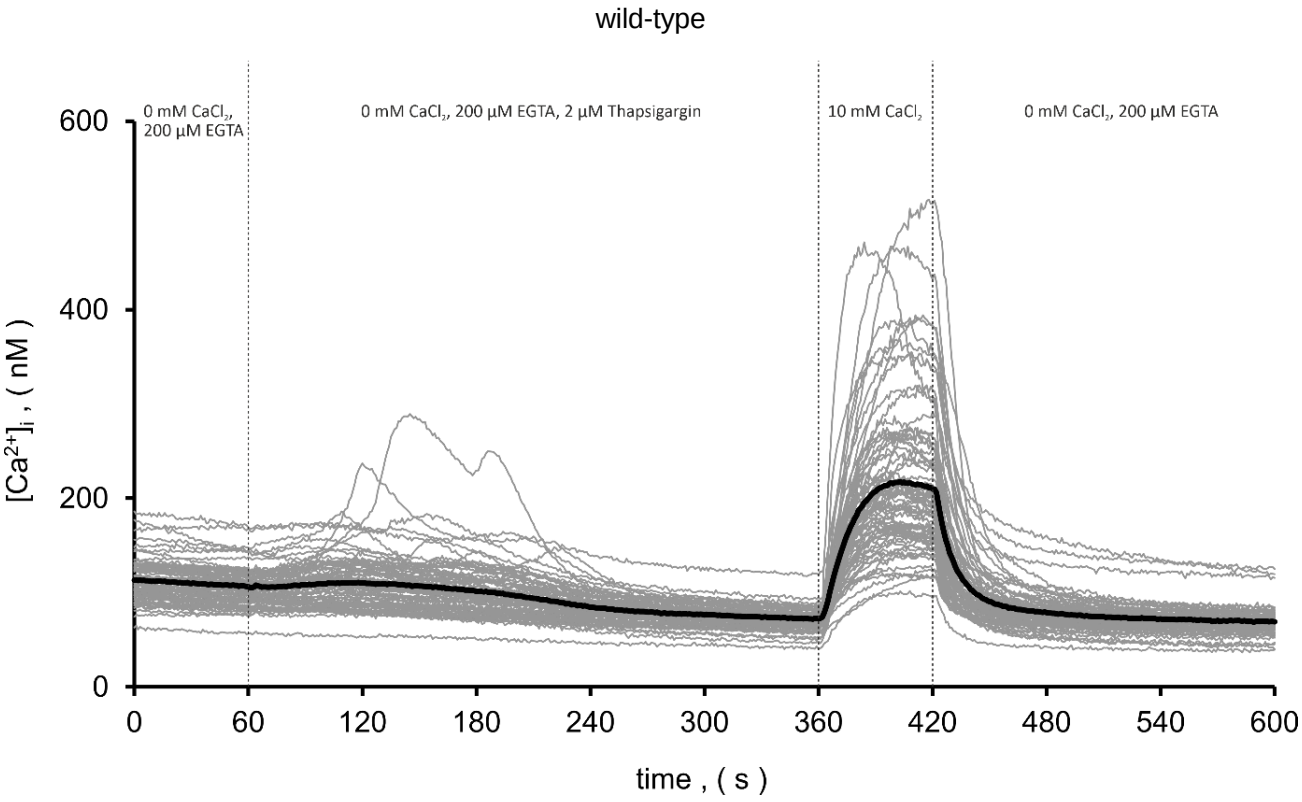

Figure S2: Detailed fluorometric $[Ca^{2+}]_i$ analysis (for details see methods) of fura-2-loaded HEK293 cells overexpressing ATP2B1 wild-type. Shown are representative recordings of $[Ca^{2+}]_i$ in 75 single cells (grey lines) and averaged signal (black line) during perfusion with various buffer conditions as indicated. Time-dependent $[Ca^{2+}]_i$ decline in Figure 4 was calculated from interval 420 s to 540 s.

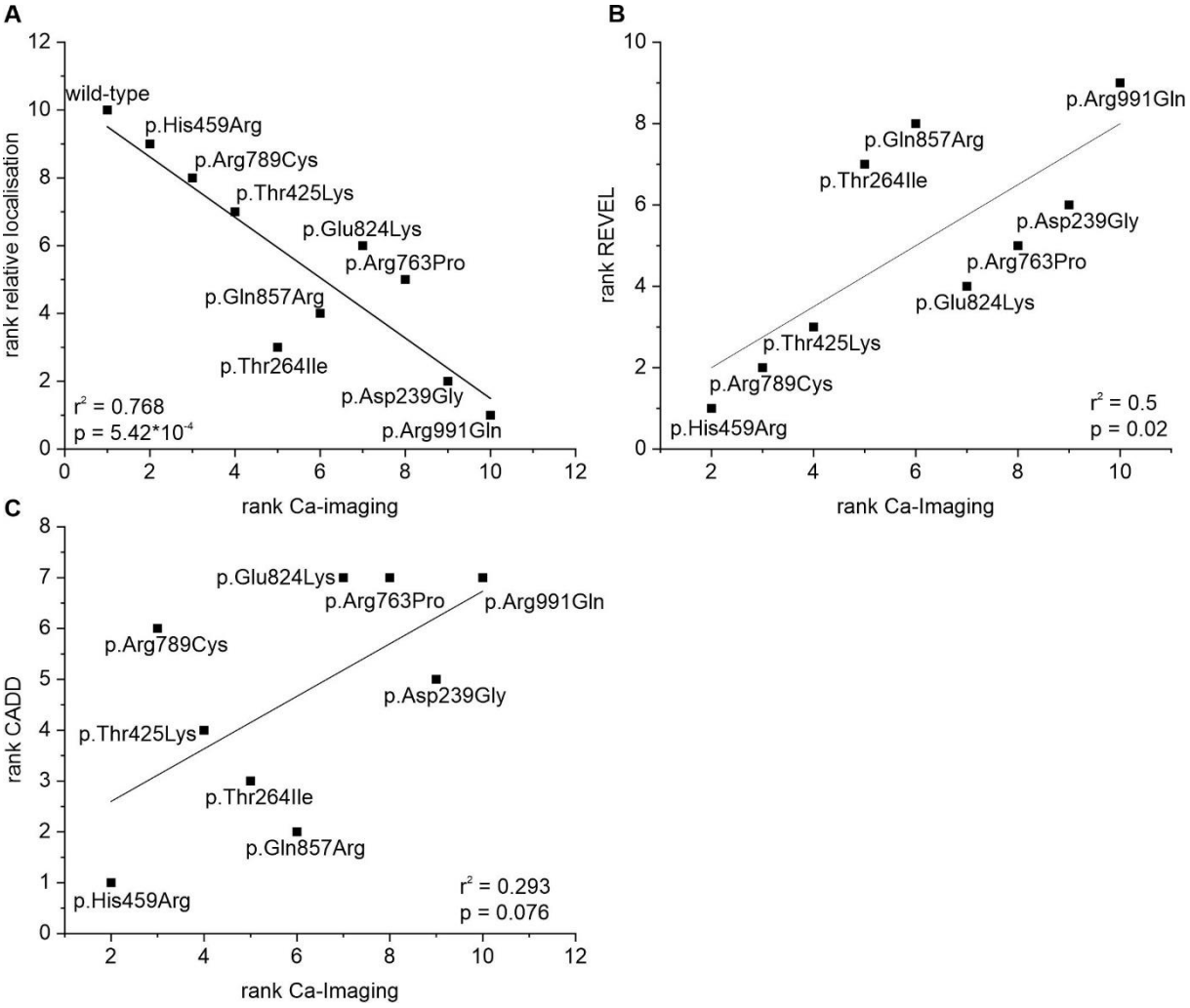

Figure S3: Correlation between tau-value, cellular localization and REVEL and CADD. (A) Correlation between $[Ca^{2+}]_i$ imaging and membrane co-localization of the *ATP2B1* variants (for details see methods) Each variant was ranked in both experiments dependent on tau-value and PCC-value. The lowest tau-value ranks at number one and the lowest PCC-value ranks as number one in relative localization. The x-axis represents the ranking of tau-value, the y-axis the ranking in relative localization. Correlation (B) between tau-value and REVEL score and (C) between tau-value and CADD score of each variant. The lowest tau-value ranks at number one again and the lowest REVEL and CADD score ranks as number one, respectively.

SUPPLEMENTAL METHODS

PATIENT STUDY

Collaborative efforts via online platforms like GeneMatcher[1] and DECIPHER[2] from different centers in Germany, the Netherlands, New Zealand, Canada, Israel, Italy, USA and France resulted into the cohort of this study. Physicians and geneticists contributed detailed clinical and genetic information, via routine clinical examination or in a research setting. In total, around 95,000 trio-exomes, exomes or genomes were analyzed in a clinical or research setting to identify 26 independent individuals with a *ATP2B1* variant. Thirteen individuals were deemed relevant and included in this study. All analyses were performed in concordance with the provisions of the German Gene Diagnostic Act (Gendiagnostikgesetz) and the General Data Protection Act (Bundesdatenschutzgesetz) for the German patients. Written informed consents of all examined individuals or their legal representatives were obtained for genetic testing and publication after advice and information about their risks and benefit. We have also collected three additional individuals that have a *de novo ATP2B1* variant, which were identified in the Deciphering Developmental Disorders Study[3]. As these variants were identified by trio-exome sequencing without further interpretation, a causal relationship of *de novo* variants in *ATP2B1* and a disorder has not been demonstrated, yet. We have not included these individuals into the clinical and variant description, as we could not acquire a detailed phenotypic description (see Figure1 and Table S1).

Sequencing, Identification and Evaluation of variants

For all cases, exome or genome sequencing were performed by using standard commercial products within a diagnostic setting. All cases were evaluated in a clinical setting and no

reportable variants were identified. After families consented for research, evaluation of the data was continued in a scientific setting. The variants were prioritized based on minor allele frequency, inheritance mode, potential predicted pathogenicity (based on several *in silico* predictions), attributes of the genes, including functional plausibility, tolerance for variants (i.e. LOEUF value and Z-Score), as well as further aspects including available animal models, interaction partners, tissue expression (the Genotype-Tissue Expression (GTEx)) and plausibility of the symptoms in regard to the function of the gene. This analysis yielded a variant in *ATP2B1* as the most promising candidate.

ATP2B1 expression plasmids

Full-length human *ATP2B1* open reading frame (ORF; GeneBank: NM_001001323.2) cDNA was obtained by PCR from healthy human brain cDNA (normal brain tissue, parietal lobe, lot. 811001, BioCat GmbH, Heidelberg, Germany) by using specific primers (Table S2) and the PfuUltra II Hotstart PCR Master Mix (Agilent Technologies, Waldbronn, Germany) according to the manufacturer's recommendation. Fragments of the *ATP2B1* ORF were amplified by PCR (Table S2) from *ATP2B1* cDNA and subcloned with the Zero Blunt TOPO PCR Cloning Kit (ThermoFisher Scientific, Darmstadt, Germany). The *ATP2B1* open-reading frame fragments were assembled by using the Golden Gate Assembly Kit (BsmBI-v2; New England Biolabs GmbH, Frankfurt am Main, Germany) according to the manufacturer's recommendation. Afterwards, the *ATP2B1* open-reading frame without a stop codon was in-frame ligated into a pcDNA3 expression vector containing the ORF of enhanced yellow fluorescent protein (YFP) by using *EcoR*I and *Xba*I restriction enzymes. Mutagenesis was performed by using the QuikChange II XL site-directed mutagenesis kit (Agilent Technologies) according to the manufacturer's recommendation. All sequences were verified by Sanger sequencing.

Cell Culture and Transfection

Transfection was performed as described previously[4]. Briefly, HEK293 cells were cultured in Eagle's Minimum Essential Medium (Sigma, Munich, Germany), supplemented with 10% fetal calf serum, 2 mM L-glutamine, 100 $U \cdot mL^{-1}$ penicillin, 0.1 $mg \cdot mL^{-1}$ streptomycin (all from Thermo Fisher Scientific) and incubated at 37°C and 5% CO_2 in humidified air in an incubator. For transfection, HEK293 cells were seeded on 25 mm glass coverslips and transfected with 4 µL JetPEI (Polyplus, Illkrich, France) and 2 µg of DNA encoding wild-type or mutated variants of ATP2B1-YFP.

Microfluorometric $[Ca^{2+}]_i$ imaging analysis

Fluorometric $[Ca^{2+}]_i$ assays in HEK293 cell lines were performed as described previously[5]. Briefly, HEK293 cells were transfected and loaded with 4 µM fura-2/AM (AAT Bioquest, Sunnyvale, California, USA) in HBS (132 mM NaCl, 6 mM KCl, 1mM $MgCl_2$, 1mM $CaCl_2$, 5.5 mM D-glucose and 10 mM HEPES, 0.1% BSA; pH 7.4) for 30 min at 37°C.

$[Ca^{2+}]_i$ measurements were performed on an inverted epifluorescence microscope with a Fluar 10×/0.5 objective (Carl Zeiss, Jena, Germany) and calibrated as described before[4, 5]. The measurements spanned 600 seconds with images taken in an interval of one second. HEK293 cells on coverslips were mounted in a bath chamber and superfused with HBS containing 200 µM EGTA. After internal Ca^{2+} store depletion with HBS containing 2 µM thapsigargin, the cells were perfused with HBS containing 10mM $CaCl_2$, followed by nominally Ca^{2+}-free HBS with 200 µM EGTA again. The time constant tau of declining $[Ca^{2+}]_i$ was calculated in GraphPad Prim 9 (Graphpad Software, Inc.; Version: 9.2.0 64-bit) by a curve fit with the function: $y=(y_0$ -

Plateau) * exp (-K * x) + Plateau, based on $[Ca^{2+}]_i$ measurements after the final addition of EGTA. The Plateau corresponds to the basal $[Ca^{2+}]_i$.

Fluorescence microscopy

HEK293 cells were transfected with the corresponding ATP2B1-YFP plasmid and with an expression plasmid that encodes a membrane-targeted cyan fluorescent protein (CAAX-box motif fused for lipid modification; CAAX). Afterwards fluorescence images were taken by using a LSM 510-META confocal laser scanning microscope (Zeiss, Jena, Germany). To determine the relative membrane localization, we analyzed the co-localization of expressed ATP2B1 and CAAX by using the EzColocalization plugin according to Stauffer *et al.* in ImageJ (version: 1.8.0_172)[6, 7]. Results are shown as Pearson correlations coefficient (PCC), which measures the correlation between pixel values for two reporter channels. A value of 0 indicates non-colocalization and a value of 1 complete co-localization.

Structural Modeling

The structural analysis of the variants was based in the cryo-EM structure of *ATP2B1* in complex with neuroplastin (PDB: 6A69[8]). Variants were modelled with Swiss-Model[9], and RasMol[10] was used for structure analysis and visualization.

Protein tolerance landscape

The tolerance landscape, as obtained by MetaDome[11], was obtained from the public available web server (https://stuart.radboudumc.nl/metadome). The algorithm maps population

variation from the Exome Aggregation Consortium (ExAC) and pathogenic variants from the Human Gene Mutation Database (HGMD) and ClinVar onto Pfam protein domains. Based on domain homology, a genetic intolerance is calculated on amino acid resolution for human protein domains.

Statistical analysis

Statistical analysis was carried out using GraphPad Prism 9 and OriginPro 2019 (version: 9.6.0.172, OriginLab, Northampton, United States). We used a one-way ANOVA with the Games-Howel post hoc test for multiple comparisons. If not stated otherwise, data is presented as mean ± standard deviation. A p-value < 0.05 was presumed to be statistically significant.

References

1. Sobreira, N., Schiettecatte, F., Valle, D., and Hamosh, A. (2015). GeneMatcher: a matching tool for connecting investigators with an interest in the same gene. Human mutation *36,* 928–930.

2. Firth, H.V., Richards, S.M., Bevan, A.P., Clayton, S., Corpas, M., Rajan, D., van Vooren, S., Moreau, Y., Pettett, R.M., and Carter, N.P. (2009). DECIPHER: Database of Chromosomal Imbalance and Phenotype in Humans Using Ensembl Resources. American journal of human genetics *84,* 524–533.

3. Kaplanis, J., Samocha, K.E., Wiel, L., Zhang, Z., Arvai, K.J., Eberhardt, R.Y., Gallone, G., Lelieveld, S.H., Martin, H.C., and McRae, J.F., et al. (2020). Evidence for 28 genetic disorders discovered by combining healthcare and research data. Nature *586,* 757–762.

4. Urban, N., Neuser, S., Hentschel, A., Köhling, S., Rademann, J., and Schaefer, M. (2017). Pharmacological inhibition of focal segmental glomerulosclerosis-related, gain of function mutants of TRPC6 channels by semi-synthetic derivatives of larixol. British journal of pharmacology *174,* 4099–4122.

5. Lenz, J.C., Reusch, H.P., Albrecht, N., Schultz, G., and Schaefer, M. (2002). Ca2+-controlled competitive diacylglycerol binding of protein kinase C isoenzymes in living cells. The Journal of cell biology *159,* 291–302.

6. Stauffer, W., Sheng, H., and Lim, H.N. (2018). EzColocalization: An ImageJ plugin for visualizing and measuring colocalization in cells and organisms. Scientific reports *8,* 15764.

7. Schneider, C.A., Rasband, W.S., and Eliceiri, K.W. (2012). NIH Image to ImageJ: 25 years of image analysis. Nature methods *9,* 671–675.

8. Gong, D., Chi, X., Ren, K., Huang, G., Zhou, G., Yan, N., Lei, J., and Zhou, Q. (2018). Structure of the human plasma membrane Ca2+-ATPase 1 in complex with its obligatory subunit neuroplastin. Nature communications *9,* 3623.

9. Guex, N., and Peitsch, M.C. (1997). SWISS-MODEL and the Swiss-PdbViewer: an environment for comparative protein modeling. Electrophoresis *18,* 2714–2723.

10. Sayle, R.A., and Milner-White, E.J. (1995). RASMOL: biomolecular graphics for all. Trends in biochemical sciences *20,* 374.

11. Wiel, L., Baakman, C., Gilissen, D., Veltman, J.A., Vriend, G., and Gilissen, C. (2019). MetaDome: Pathogenicity analysis of genetic variants through aggregation of homologous human protein domains. Human mutation *40,* 1030–1038.